

ShOpt.jl | A Julia Library for Empirical Point Spread Function Characterization of JWST NIRCам Data

Edward Berman¹ and Jacqueline McCleary¹

¹ Northeastern University, USA ¶ Corresponding author

DOI: [10.xxxxxx/draft](https://doi.org/10.xxxxxx/draft)

Software

- [Review](#)
- [Repository](#)
- [Archive](#)

Editor: [Open Journals](#)

Reviewers:

- [@openjournals](#)

Submitted: 01 January 1970

Published: unpublished

License

Authors of papers retain copyright and release the work under a Creative Commons Attribution 4.0 International License ([CC BY 4.0](#))

In partnership with



AMERICAN
ASTRONOMICAL
SOCIETY

This article and software are linked with research article DOI [10.3847/xxxxx](https://doi.org/10.3847/xxxxx), published in the *Astronomical Journal*.

Summary

Introduction

When astronomers image the night sky, the path of the incoming light has been altered by diffraction, optical aberrations, atmospheric turbulence, and telescope jitter. These effects are summarized in the image's point spread function (PSF), a mathematical model that describes the response of an optical system to an idealized point of light. Because the PSF can resemble or obscure the signal of interest, it must be carefully modeled to extract the maximum amount of information from an observation. Failing to do so can lead to inaccuracies in positions, sizes, and shapes of targets like galaxies.

The goal of PSF characterization is to be able to point to any position on your camera and predict what the distortion looks like. Once we have a model that can do this well, we can deconvolve the PSF to produce images free of distortion.

The PSF characterization methods used by astronomers fall into two main classes: forward-modeling approaches, which use physical optics propagation based on models of the optical array, and empirical approaches, which use stars as fixed points to model and interpolate the PSF across the rest of the image. (Stars are essentially point sources before their light passes through the atmosphere and telescope, so the shape and size of their surface brightness profiles axiomatically define the PSF at that location.) Empirical PSF characterization proceeds by first cataloging the observed stars, separating the catalog into validation and training samples, and interpolating the training stars across the field of view of the camera. We use the term vignets to describe the image stamps containing stars that make up the catalog. After training, the PSF model can be validated by comparing the reserved stars to the PSF model's prediction.

Shear Optimization with ShOpt.jl introduces modern techniques for empirical PSF characterization across the field of view that are tailored to James Webb Space Telescope (JWST) imaging. ShOpt has two modes of operation: approximating stars with analytic profiles, and a more realistic pixel-level representation.

Analytic profile mode

A rough idea of the size and shape of the PSF can be obtained by fitting stars with analytic profiles. We adopt a multivariate Gaussian profile because it is computationally cheap to fit to an image. That is, it is easy to differentiate and doesn't involve any numeric integration or other costly steps to calculate. Fitting other common models, such as a Kolmogorov profile, involves numeric integration and thus take much longer to fit. Moreover, the JWST point spread function is very "spikey" (cf. Figure 1). As a result, analytic profiles are limited in their ability to model the point spread function anyway, making the usual advantages of a more expensive analytic profile moot.

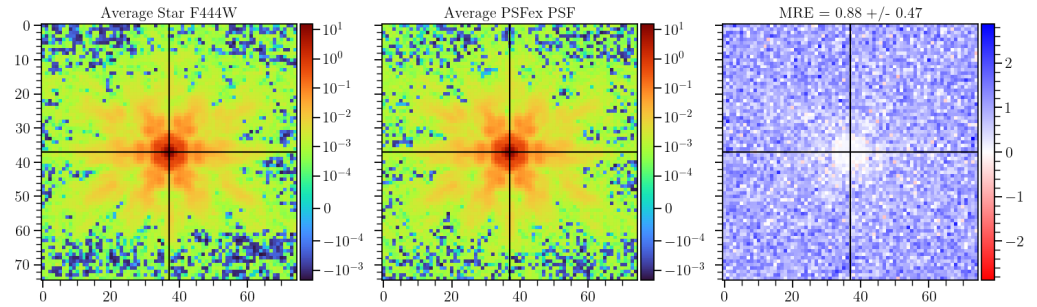


Figure 1: The plot on the left shows the average cutout of all of the stars in a supplied catalog. Likewise, plot in the middle shows the average point spread function model. The plot on the right shows the average normalized error between the observed star cutouts and the point spread function model.

Our multivariate gaussian is parameterized by three variables, $[s, g_1, g_2]$, where s corresponds to size and g_1, g_2 correspond to shear. A shear matrix has the form

$$\begin{pmatrix} 1 + g_1 & g_2 \\ g_2 & 1 - g_1 \end{pmatrix}$$

. Given a point $[u, v]$, we obtain coordinates $[u', v']$ by applying a shear and then a scaling by $\frac{s}{\sqrt{1-g_1^2-g_2^2}}$. Then, we choose $f(r) := Ae^{-r^2}$ to complete our fit, where A makes the fit sum to unity over the cutout of our star. After we fit this function to our stars with `Optim.jl` (Mogensen & Riseth, 2018) and `ForwardDiff.jl` (Revels et al., 2016), we interpolate the parameters across the field of view according to position. Essentially, each star is a datapoint, and the three variables are treated as polynomials in focal plane coordinates (u, v) of degree n , where n is supplied by the user. The focal plain refers to the set of points where an image appears to be in perfect focus. The units of focal plane coordinates are arcseconds. This is instead of pixel coordinates, where one just uses (x, y) as measured on an image. For a more precise model, we also give each pixel in our star stamp a polynomial and interpolate it across the field of view. That is, each pixel in position (i, j) of a star cutout gets its own polynomial, interpolated over k different star cutouts at different locations in the focal plane. This is referred to in the literature as a pixel basis (Jarvis et al., 2020).

Notation

1. For the set $B_2(r)$, we have:

$$B_2(r) \equiv \{[x, y] : x^2 + y^2 < 1\} \subset \mathbb{R}^2$$

2. For the set \mathbb{R}_+ , we have:

$$\mathbb{R}_+ \equiv \{x : x > 0\} \subset \mathbb{R}$$

3. For the Cartesian product of sets A and B , we have:

$$A \times B \equiv \{(a, b) : a \in A, b \in B\}$$

59 Analytic methods

60 ShOpt.jl's analytic profile fitting takes inspiration from a number of algorithms outside
61 of astronomy, notably SE-Sync (Rosen et al., 2019), an algorithm that solves the robotic
62 mapping problem by considering the manifold properties of the data. With sufficiently clean
63 data, the SE-Sync algorithm will descend to a global minimum constrained to the manifold
64 $SE(d)^n/SE(d)$. Following suit, we are able to put a constraint on the solutions we obtain
65 to $[s, g_1, g_2]$ to a manifold. The solution space to $[s, g_1, g_2]$ is constrained to the manifold
66 $B_2(r) \times \mathbb{R}_+$ (Bernstein & Jarvis, 2002). While it was known that this constrain existed in
67 the literature, the parameter estimation task is generally framed as an unconstrained problem
68 (Jarvis et al., 2020). For a more rigorous treatment of optimization on manifolds see (Absil
69 et al., 2008) and (Boumal, 2023). Julia has lots of support for working with manifolds with
70 Manopt, which we may leverage in future releases (Bergmann, 2022).

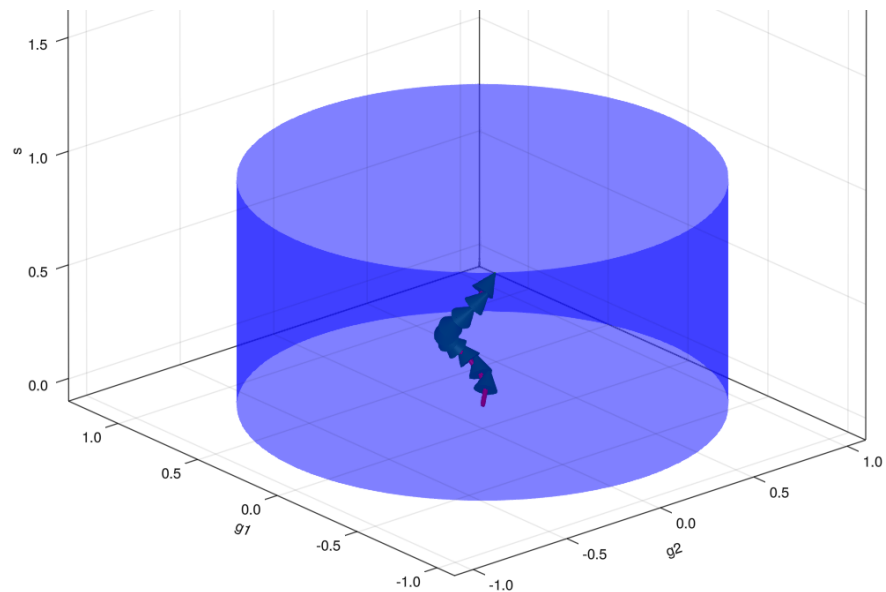


Figure 2: LFBGS algorithm used to find parameters subject to the cylindrical constraint. s is arbitrarily capped at 1 as a data cleaning method.

71 Pixel grid mode

72 ShOpt.jl provides two modes for pixel grid fits, PCA mode and Autoencoder mode. PCA mode,
73 outlined below, reconstructs its images using the first n principal components. Autoencoder
74 mode uses a neural network to reconstruct the image from a lower dimensional latent space.
75 The network code written with Flux.jl is also outlined below (Innes, 2018). Both modes
76 provide the end user with tunable parameters that allow for both perfect reconstruction of
77 star cutouts and low dimensional representations. The advantage of these modes is that they
78 provide good reconstructions of the distorted images that can learn the key features of the
79 point spread function without overfitting the background noise. In this way it generates a
80 datapoint for our algorithm to train on and denoises the image in one step. In both cases, the
81 input star data is cleaned by first fitting an analytic (Gaussian) PSF profile and rejecting size
82 outliers.

83 Pixel methods

84 PCA mode

```
function pca_image(image, ncomponents)
    #Load img Matrix
```

```

img_matrix = image

# Perform PCA
M = fit(PCA, img_matrix; maxoutdim=ncomponents)

# Transform the image into the PCA space
transformed = MultivariateStats.transform(M, img_matrix)

# Reconstruct the image
reconstructed = reconstruct(M, transformed)

# Reshape the image back to its original shape
reconstructed_image = reshape(reconstructed, size(img_matrix)...)
end

85 Autoencoder mode

# Encoder
encoder = Chain(
    Dense(r*c, 128, leakyrelu),
    Dense(128, 64, leakyrelu),
    Dense(64, 32, leakyrelu),
)

#Decoder
decoder = Chain(
    Dense(32, 64, leakyrelu),
    Dense(64, 128, leakyrelu),
    Dense(128, r*c, tanh),
)

#Full autoencoder
autoencoder = Chain(encoder, decoder)

#x_hat = autoencoder(x)
loss(x) = mse(autoencoder(x), x)

# Define the optimizer
optimizer = ADAM()

```

86 Statement of need

87 We can trace the first empirical PSF fitters back to DAOPHOT (Stetson, 1987). PSFex made
 88 major advancements in precise PSF modeling. With PSFex, you could interpolate several
 89 different bases, including a basis of pixels, instead of relying on simple parametric functions.
 90 PSFex was built as a general purpose tool and to this day is widely used. Newer empirical
 91 PSF fitters are geared toward large scale surveys and the difficulties that arise specific to
 92 those datasets. As an example, The Dark Energy Survey and DESCam (Flaugher et al., 2015;
 93 Jarvis et al., 2020) sparked the creation of PIFF. The recent data from the James Webb Space
 94 Telescope poses new challenges.

- 95 (1) The JWST PSFs are not well approximated by analytic profiles as seen in Figure 1. This
 96 calls for well thought out parametric free models that can capture the full dynamic range
 97 of the Point Spread Function without fixating on the noise in the background. Previously,
 98 Rowe statistics and other parametric equations were used to diagnose PSF accuracy
 99 (Rowe, 2010). ShOpt provides a suite of parametric free summary statistics out of the
 100 box.

(2) The NIRC2 detectors are $0.03''/\text{pix}$ or $0.06''/\text{pix}$ (Beichman et al., 2012a; Rieke et al., 2003, 2005). To capture an accurate description of the point spread function at this scale we need images that are 131 by 131 to 261 by 261 pixels across. These vignette sizes are much larger in comparison to the sizes needed for previous large surveys such as DES (Jarvis et al., 2020) and SuperBIT (McCleary et al., 2023) and forces us to evaluate how well existing PSF fitters scale to this size. The DES and SuperBIT surveys needed PSF sizes of 17 by 17 and 48 by 48, an order of magnitude less than the JWST PSF sizes.

109 **State of the Field**

There are several existing empirical PSF fitters in addition to a forward model of the JWST PSFs developed by STScI (Jarvis et al., 2020; Bertin, 2011; Perrin et al., 2014; Perrin et al., 2012). We describe them here and draw attention to their strengths and weaknesses to motivate the development of Sh0pt.jl. As described in the statement of need, PSFex was one of the first precise and general purpose tools used for empirical PSF fitting. However, PSFex produced a systematic size bias of the point spread function with how it calculated spatial variation across the field of view (Jarvis et al., 2020). It was discovered via the analytic profile fits that the size of the point spread function, governed by the variable $[s]$, was underestimated.

PIFF (Point Spread Functions in the Full Field of View) followed PSFex in the effort to correct this issue. The DES camera was 2.2 degrees across, which was large enough for the size bias to become noticable for their efforts. PIFF works in focal plane coordinates as opposed to pixel coordinates which fixes the systematic size bias. Jarvis and DES also used the Python libraries of astropy (Astropy Collaboration et al., 2022) and Galsim (Rowe et al., 2015) to make the software more accessible than PSFex to programmers in the astrophysics community. PSFex was written in C and has been active for more than 20 years. Due to being so old and written in a low level language it is much less approachable for a community of open source developers. One of the motivations of Sh0pt was to write astrophysics specific software in Julia, because Julia provides a nice balance of readability and speed with it's high level functional paradigm and just in time compiler. Sh0pt works directly in sky coordinates, which minimizes any bias that might be introduced by transformation from pixel to sky coordinates afterwards.

While we do have forwards models of the JWST PSF, these models are for single exposure images. The JWST images are either single exposure or mosaics (Perrin et al., 2014, 2012). Mosaiced images are essentially single exposure detector images averaged together. To account for the rotation of the camera between the capture of images and the wide field of view, there are a number of steps that make applying these forward models to mosaics a non trivial procedure. There is also some recent work being done to generate hybrid models for single exposure data (Lin et al., 2023). Hybrid models take these forward models and add an empirical correction. At present, there is yet to be any widely available software to do this.

The COMOS-Web survey is the largest JWST extragalactic survey according to area and prime time allocation (Casey et al., 2023), and takes up 0.54 deg^2 (Beichman et al., 2012b; Rieke et al., 2023). This is a large enough portion of the sky that we should prepare to see a lot of variation across the field of view. This gives Sh0pt the opportunity to validate PIFF's correction for handling PSF variations and test how impactful (or not impactful) PSFex's size bias is.

144 **Future Work**

We speculate that petal diagrams may be able to approximate the spikey natures of JWST PSFS. Consider $r = A \cos(k\theta + \gamma)$, shown below in figure 3 for different $[A, k]$ values where $\gamma = 0$. In practice, $[A, k, \gamma]$ could be learnable parameters. Moreover, we could do this for a series of trigonometric functions to get petals of different sizes. We could then choose some

149 $f(r) \propto \frac{1}{r}$ such that the gray fades from black to white. We would define $f(r)$ piece wise such
150 that it is 0 outside of the petal and decreases radially with r inside the petal.

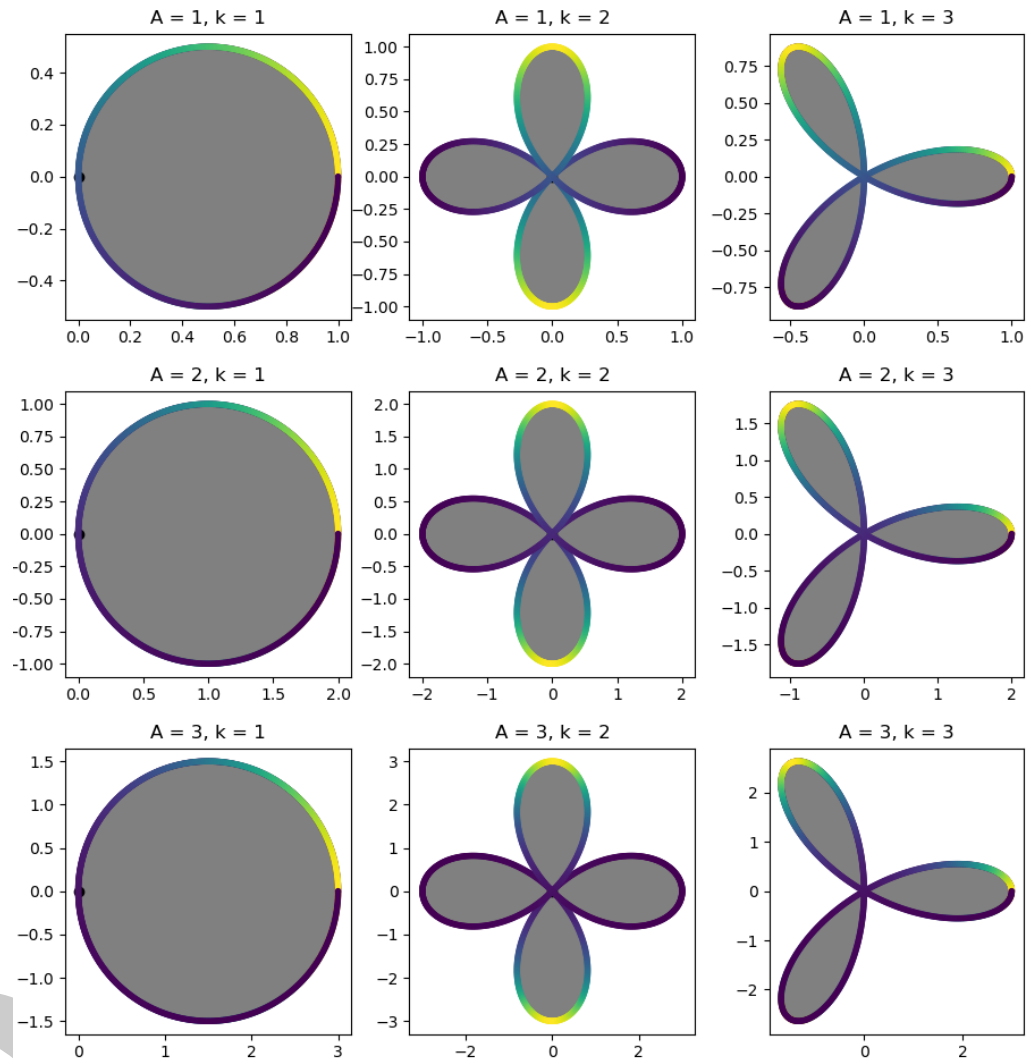


Figure 3: Petal Diagram

Acknowledgements

151 This material is based upon work supported by a Northeastern University Undergraduate Re-
152 search and Fellowships PEAK Experiences Award. We would also like to thank the Northeastern
153 Physics Department for making this project possible through the Physics Co-op Research
154 Fellowship. Support for COSMOS-Web was provided by NASA through grant JWST-GO-01727
155 and HST-AR-15802 awarded by the Space Telescope Science Institute, which is operated by the
156 Association of Universities for Research in Astronomy, Inc., under NASA contract NAS 5-26555.
157 This work was made possible by utilizing the CANDIDE cluster at the Institut d'Astrophysique
158 de Paris. Finally, we would like to thank Northeastern Research Computing for access to their
159 servers. Additionally, we'd like to extend a thank you to Professor David Rosen for giving some
160 valuable insights during the early stages of this work.
161

References

- Absil, P.-A., Mahony, R., & Sepulchre, R. (2008). *Optimization algorithms on matrix manifolds* (p. xvi+224). Princeton University Press. ISBN: 978-0-691-13298-3
- Astropy Collaboration, Price-Whelan, A. M., Lim, P. L., Earl, N., Starkman, N., Bradley, L., Shupe, D. L., Patil, A. A., Corrales, L., Brasseur, C. E., Nöthe, M., Donath, A., Tollerud, E., Morris, B. M., Ginsburg, A., Vaher, E., Weaver, B. A., Tocknell, J., Jamieson, W., ... Astropy Project Contributors. (2022). The Astropy Project: Sustaining and Growing a Community-oriented Open-source Project and the Latest Major Release (v5.0) of the Core Package. *935*(2), 167. <https://doi.org/10.3847/1538-4357/ac7c74>
- Beichman, C. A., Rieke, M., Eisenstein, D., Greene, T. P., Krist, J., McCarthy, D., Meyer, M., & Stansberry, J. (2012b). Science opportunities with the near-IR camera (NIRCam) on the James Webb Space Telescope (JWST). In M. C. Clampin, G. G. Fazio, H. A. MacEwen, & J. M. O. Jr. (Eds.), *Space telescopes and instrumentation 2012: Optical, infrared, and millimeter wave* (Vol. 8442, p. 84422N). International Society for Optics; Photonics; SPIE. <https://doi.org/10.1117/12.925447>
- Beichman, C. A., Rieke, M., Eisenstein, D., Greene, T. P., Krist, J., McCarthy, D., Meyer, M., & Stansberry, J. (2012a). Science opportunities with the near-IR camera (NIRCam) on the James Webb Space Telescope (JWST). In M. C. Clampin, G. G. Fazio, H. A. MacEwen, & Jr. Oschmann Jacobus M. (Eds.), *Space telescopes and instrumentation 2012: Optical, infrared, and millimeter wave* (Vol. 8442, p. 84422N). <https://doi.org/10.1117/12.925447>
- Bergmann, R. (2022). Manopt.jl: Optimization on manifolds in Julia. *Journal of Open Source Software*, *7*(70), 3866. <https://doi.org/10.21105/joss.03866>
- Bernstein, G. M., & Jarvis, M. (2002). Shapes and shears, stars and smears: Optimal measurements for weak lensing. *The Astronomical Journal*, *123*(2), 583. <https://doi.org/10.1086/338085>
- Bertin, E. (2011). Automated Morphometry with SExtractor and PSFEx. In I. N. Evans, A. Accomazzi, D. J. Mink, & A. H. Rots (Eds.), *Astronomical data analysis software and systems XX* (Vol. 442, p. 435).
- Boumal, N. (2023). *An introduction to optimization on smooth manifolds*. Cambridge University Press. <https://doi.org/10.1017/9781009166164>
- Casey, C. M., Kartaltepe, J. S., Drakos, N. E., Franco, M., Harish, S., Paquereau, L., Ilbert, O., Rose, C., Cox, I. G., Nightingale, J. W., Robertson, B. E., Silverman, J. D., Koekemoer, A. M., Massey, R., McCracken, H. J., Rhodes, J., Akins, H. B., Amvrosiadis, A., Arango-Toro, R. C., ... Zavala, J. A. (2023). *COSMOS-web: An overview of the JWST cosmic origins survey*. <https://arxiv.org/abs/2211.07865>
- Flaugher, B., Diehl, H. T., Honscheid, K., Abbott, T. M. C., & others. (2015). The dark energy camera. *AJ*, *150*, 150. <https://doi.org/10.1088/0004-6256/150/5/150>
- Innes, M. (2018). Flux: Elegant machine learning with julia. *Journal of Open Source Software*. <https://doi.org/10.21105/joss.00602>
- Jarvis, M., Bernstein, G. M., Amon, A., Davis, C., Lé get, P. F., Bechtol, K., Harrison, I., Gatti, M., Roodman, A., Chang, C., Chen, R., Choi, A., Desai, S., Drlica-Wagner, A., Gruen, D., Gruendl, R. A., Hernandez, A., MacCrann, N., Meyers, J., ... and, R. D. W. (2020). Dark energy survey year 3 results: Point spread function modelling. *Monthly Notices of the Royal Astronomical Society*, *501*(1), 1282–1299. <https://doi.org/10.1093/mnras/staa3679>
- Lin, Nie, Huanyuan, Shan, Guoliang, Li, Lei, Wang, Charling, Tao, Qifan, Cui, Yushan, Xie, Dezi, Liu, Zekang, & Zhang. (2023). *HybPSF: Hybrid PSF reconstruction for the observed JWST NIRCam image*. <https://arxiv.org/abs/2308.14065>

- McCleary, J. E., Everett, S. W., Shaaban, M. M., Gill, A. S., Vassilakis, G. N., Huff, E. M., Massey, R. J., Benton, S. J., Brown, A. M., Clark, P., & others. (2023). Lensing in the blue II: Estimating the sensitivity of stratospheric balloons to weak gravitational lensing. *arXiv Preprint arXiv:2307.03295*.
- Mogensen, P. K., & Riseth, A. N. (2018). Optim: A mathematical optimization package for julia. *Journal of Open Source Software*, 3(24), 615. <https://doi.org/10.21105/joss.00615>
- Perrin, M. D., Sivaramakrishnan, A., Lajoie, C.-P., Elliott, E., Pueyo, L., Ravindranath, S., & Albert, Loic. (2014). Updated point spread function simulations for JWST with WebbPSF. In Jr. Oschmann Jacobus M., M. Clampin, G. G. Fazio, & H. A. MacEwen (Eds.), *Space telescopes and instrumentation 2014: Optical, infrared, and millimeter wave* (Vol. 9143, p. 91433X). <https://doi.org/10.1117/12.2056689>
- Perrin, M. D., Soummer, R., Elliott, E. M., Lallo, M. D., & Sivaramakrishnan, A. (2012). Simulating point spread functions for the James Webb Space Telescope with WebbPSF. In M. C. Clampin, G. G. Fazio, H. A. MacEwen, & Jr. Oschmann Jacobus M. (Eds.), *Space telescopes and instrumentation 2012: Optical, infrared, and millimeter wave* (Vol. 8442, p. 84423D). <https://doi.org/10.1117/12.925230>
- Revels, J., Lubin, M., & Papamarkou, T. (2016). Forward-mode automatic differentiation in Julia. *arXiv:1607.07892 [Cs.MS]*. <https://arxiv.org/abs/1607.07892>
- Rieke, M. J., Baum, S. A., Beichman, C. A., Crampton, D., Doyon, R., Eisenstein, D., Greene, T. P., Hodapp, K.-W., Horner, S. D., Johnstone, D., Lesyna, L., Lilly, S., Meyer, M., Martin, P., Jr., D. W. M., Rieke, G. H., Roellig, T. L., Stauffer, J., Trauger, J. T., & Young, E. T. (2003). NGST NIRCам scientific program and design concept. In J. C. Mather (Ed.), *IR space telescopes and instruments* (Vol. 4850, pp. 478–485). International Society for Optics; Photonics; SPIE. <https://doi.org/10.1117/12.489103>
- Rieke, M. J., Kelly, D. M., Misselt, K., Stansberry, J., Boyer, M., Beatty, T., Egami, E., Florian, M., Greene, T. P., Hainline, K., Leisenring, J., Roellig, T., Schlawin, E., Sun, F., Tinnin, L., Williams, C. C., Willmer, C. N. A., Wilson, D., Clark, C. R., ... Young, E. T. (2023). Performance of NIRCам on JWST in flight. *Publications of the Astronomical Society of the Pacific*, 135(1044), 028001. <https://doi.org/10.1088/1538-3873/acac53>
- Rieke, M. J., Kelly, D., & Horner, S. (2005). Overview of James Webb Space Telescope and NIRCам's Role. In J. B. Heaney & L. G. Burriesci (Eds.), *Cryogenic optical systems and instruments XI* (Vol. 5904, pp. 1–8). <https://doi.org/10.1117/12.615554>
- Rosen, D. M., Carbone, L., Bandeira, A. S., & Leonard, J. J. (2019). SE-sync: A certifiably correct algorithm for synchronization over the special euclidean group. *The International Journal of Robotics Research*, 38(2-3), 95–125. <https://doi.org/10.1177/0278364918784361>
- Rowe, B. (2010). Improving PSF modelling for weak gravitational lensing using new methods in model selection. *404*(1), 350–366. <https://doi.org/10.1111/j.1365-2966.2010.16277.x>
- Rowe, B., Jarvis, M., Mandelbaum, R., Bernstein, G. M., Bosch, J., Simet, M., Meyers, J. E., Kacprzak, T., Nakajima, R., Zuntz, J., Miyatake, H., Dietrich, J. P., Armstrong, R., Melchior, P., & Gill, M. S. S. (2015). *GalSim: The modular galaxy image simulation toolkit*. <https://arxiv.org/abs/1407.7676>
- Stetson, P. B. (1987). DAOPHOT: A COMPUTER PROGRAM FOR CROWDED-FIELD STELLAR PHOTOMETRY. *Publications of the Astronomical Society of the Pacific*, 99(613), 191. <https://doi.org/10.1086/131977>